

Screening length in compensation-doped semiconductors and topological insulators

Jonathan Lux, Qingyufei Terenz Feng, and Achim Rosch*

Institute for Theoretical Physics, University of Cologne, D-50937 Cologne, Germany

(Dated: June 10, 2022)

In most semiconductors and insulators the presence of a small density of charged impurities cannot be avoided, but their effect can be reduced by compensation doping, i.e. by introducing defects of opposite charge. Screening in such a system leads to the formation of electron-hole puddles, which dominate bulk transport properties, as first recognized by Efros and Shklovskii. We investigate the screening length ℓ_s , which determines the distance of puddles, in the limit where the gap Δ is much larger than the typical Coulomb energy E_c of neighboring dopants, $\Delta \gg E_c$. In particular, this is relevant for three dimensional Bi-based topological insulators, which typically have a large dielectric constant. Scaling arguments predict $\ell_s \sim (\Delta/E_c)^2$. In contrast, we find numerically that $\ell_s \sim (\Delta/E_c)^\gamma$ with $\gamma \approx 1.1 \pm 0.1$ is much smaller and argue that the breakdown of scaling is associated to overscreening. In topological insulators the surface state provides an additional screening channel suppressing puddle formation in a region of width ℓ_s close to the surface, strongly affecting the properties of thin slabs of topological insulators.

I. INTRODUCTION

The formation of locally conducting puddles is a phenomenon caused by charged Coulomb disorder in insulators, semiconductors and Dirac-matter like graphene, topological surface states or Weyl semi metals. Efros and Shklovskii [1] predicted that puddle formation is, in three dimensions, an unavoidable consequence of the long-range nature of the Coulomb interaction. Puddles are formed to screen large potential fluctuations exceeding the size of the gap Δ .

In graphene it has been shown both theoretically and experimentally that puddles are necessary to understand most transport experiments close to charge neutrality [2–5]. Recently, they have been observed for the first time in the bulk of a three-dimensional topological insulator [6, 7]. These materials, from the class of the $\text{Bi}_{2-x}\text{Sb}_x\text{Te}_{3-y}\text{Se}_y$ compounds [8], are almost perfectly compensated semiconductors with a band gap of order 250–300 meV. The relatively high density ($> 10^{19}\text{cm}^{-3}$) of dopants implies a strongly fluctuating Coulomb potential in the bulk. This leads to band bending and eventually to the formation of electron and hole puddles [9, 10]. The additional surface states in the topological materials induce an additional screening channel close to surface. Here surface puddles form [10, 11] which are akin to puddles that form in graphene on a substrate which has charged impurities.

As the puddles are separated by insulating regions, they do not directly contribute to the DC conductivity. However, they do contribute to the optical conductivity at finite frequencies, which has been used to detect their presence and to measure the effective charge density in conducting regions [6]. We have shown that screening from thermal excitations can efficiently suppress puddle formation leading to a characteristic temperature depen-

dence of the optical response [6]. Furthermore, in similar compounds a giant negative magnetoresistance was found experimentally and explained by merging of puddles driven by the Zeeman effect [12].

Surface puddles and puddles in graphene can be observed directly in real space by scanning tunneling microscopy (STM) [4, 5, 13]. From the two-dimensional STM maps, the size of the potential fluctuations and the corresponding length scale can be directly read off. These agree well with theoretical results, where these quantities are calculated self-consistently [2, 3, 11]. However, nothing is known experimentally about the length scales of puddles in the bulk and the effect of surface screening on the bulk puddle formation.

In the following we demonstrate numerically that the length scales governing both, the screening and the puddle formation, are much smaller than can be expected from scaling arguments. First we introduce the model and consider the scaling behavior of the charge-charge correlation function. We show numerical results for the bulk, and demonstrate that the simple scaling theory fails. Then we additionally take into account the gapless surface states which provide an extra screening channel. The length scales governing the size of puddles on the surface is different, and independent of the bulk band gap [11]. The bulk screening length describes, however, the size of a region where surface screening suppresses the formation of bulk puddles and is therefore important to understand the properties of thin topological insulator samples.

II. MODEL AND SIMULATIONS

Bi-based topological insulators typically have a very large dielectric constant $\epsilon \approx 200$. Electron binding energies are therefore small. Thus, the bare energies of the dopants are located very close to the band edges and can be approximated by $+\Delta/2$ for the donors and $-\Delta/2$ for the acceptors. To model the non-linear screening of ran-

* rosch@thp.uni-koeln.de

domly placed charged impurities in such a system we use a simple classical model [6, 9, 10, 14]:

$$H = H_n + H_C = \frac{\Delta}{2} \sum_i f_i n_i + \frac{1}{2} \sum_{i \neq j} V_{ij} q_i q_j. \quad (1)$$

where $f_i = \pm 1$ are random numbers with $f_i = +1$ for a donor states and $f_i = -1$ for the acceptor state at position \mathbf{r}_i . V_{ij} denotes the Coulomb interaction between the dopants at positions \mathbf{r}_i and \mathbf{r}_j . $n_i \in \{0, 1\}$ denotes the electronic occupation of the i -th dopant and is determined by minimizing the Hamiltonian. It is related to its charge q_i (in units of $|e|$ where e is the electron charge) by

$$q_i = \frac{f_i + 1}{2} - n_i. \quad (2)$$

A donor (acceptor) in its ground state is characterized by $f_i = 1$, $n_i = 0$ and $q_i = 1$ ($f_i = -1$, $n_i = 1$, $q_i = -1$). Somewhat counter-intuitively, screening occurs when the Coulomb interaction drives donors or acceptors into a neutral states with $q_i = 0$. Several neutral donor states close by form an electron puddle, while neighboring neutral acceptor states form hole puddles. The Coulomb energy is modeled by

$$V_{ij} = \frac{e^2}{4\pi\epsilon\epsilon_0\sqrt{|\mathbf{r}_i - \mathbf{r}_j|^2 + a_B^2}} = \frac{E_c}{\sqrt{|\mathbf{x}_i - \mathbf{x}_j|^2 + 1^2}} \quad (3)$$

Here the short-distance cutoff $a_B = \frac{4\pi\epsilon_0\epsilon}{m^*e^2}$ was introduced by Skinner *et. al.* [9, 10] to take into account that the wave function of the bound state is smeared over a length scale set by the effective Bohr radius of the impurity state. Skinner *et. al.* [9, 10] argued that due to the large dielectric constant in Bi based topological insulators, a_B is large and of similar size as the typical distance of dopants. We use $a_B = N^{-1/3}$ where $N = N_A = N_D$ is the density of dopants where we assume a perfectly compensated system where the density of donors equals the density of acceptors $N_A = N_D$. For the last equality in Eq. (3) we expressed all distance in units of the average dopant distance $N^{-1/3}$. Here

$$E_c = \frac{e^2 N^{1/3}}{4\pi\epsilon\epsilon_0}. \quad (4)$$

is the typical energy scale describing the Coulomb interaction of neighboring dopants. A large $\epsilon \sim 200$ leads to a small energy scale $E_c \sim 3.3 \text{ meV} \sim 40 \text{ K}$, (assuming a typical density $N = 10^{20} \text{ cm}^{-3}$) about 2 orders of magnitude smaller than typical band gaps Δ . Indeed, in Ref. [6] we used the temperature dependence of the optical response to determine E_c and found $\Delta/E_c \approx 150$. In the following we assume $T \ll E_c \ll \Delta$ and consider therefore only properties at $T = 0$.

The model (1) describes how donor and acceptor states interact with each other. It does not include the states in the electronic bands. This turns out [6] to be well

justified in the limit $\Delta/E_c \gg 1$ as the density of the relevant electronic states is much smaller than the density of dopants in this limit.

To find the true ground state of the model in Eq. (1) is an exponentially hard problem, but there is an algorithm to find an approximate ground state, called a pseudo ground state, in polynomial time [1, 9]. The physical properties of a pseudo ground state are expected to be indistinguishable from that of the true ground state. The single particle energies are defined as

$$\epsilon_j = \frac{\Delta}{2} f_j - \phi_j = \frac{\Delta}{2} f_j - \sum_{i \neq j} V_{ij} q_i. \quad (5)$$

In a pseudo ground state

$$\Delta E_{(\alpha,\beta)} = \epsilon_\beta - \epsilon_\alpha - V_{\alpha\beta} > 0 \quad (6)$$

has to be fulfilled for all pairs with $n_\beta = 0, n_\alpha = 1$. This state can be reached by exchanging electrons between states where this condition is not met. The algorithm is described in detail in Refs. [9, 10]. Simulations are performed in a cubic volume $V = L^3$ with periodic boundary conditions with $2L^3$ dopants, typically we use $L = 50$ or $L = 60$ corresponding to 250000 or 432000 dopants. Numerical results shown below are averaged over 200 – 800 disorder realizations, i. e. random configurations of the dopant positions. We have checked [15] that our code reproduces published results (e.g. on the Coulomb gap in the density of states) from other groups [9] on the same model in all quantitative details. In the following we use dimensionless units where all length are measured in units of $N^{-1/3}$, and all energies are measured in units of E_c defined in Eq. (4). In these units the only free parameter of our model is Δ .

III. SCALING

One of the main question that we will address is the following: What is the typical distance between electron and hole puddles or, equivalently, on what length scale does the potential typically change by an amount of Δ ? It turns out that this length scale is identical to the screening length, defined more precisely below.

A simple scaling argument by Efros and Shklovskii [16] suggests that the corresponding length scales as $R_g \sim \Delta^2$. The argument is as follows: in a volume of size $V \sim R^3$ there are on average NR^3 positive and negative charges where N is the density of dopants. But these two numbers are not exactly equal, instead the typical charge of the region is (in the uncorrelated state) $Q_R \sim \pm\sqrt{NR^3}$. This implies a typical potential of order $\phi_R \sim Q_R/R \sim \sqrt{R}$ within that region. The fact that this potential diverges for $R \rightarrow \infty$ shows that this situation is unstable and the huge potential fluctuations have to be screened. The potential can be screened when the Coulomb potential is sufficiently strong to change the charging state of the dopant. This is possible for

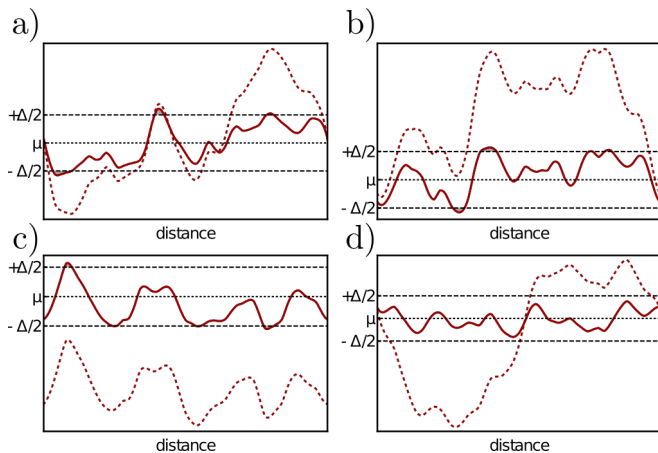


Figure 1. (Color online) Due to charged impurities, the potential fluctuates in space. Huge fluctuations of the potential in the uncorrelated state (dashed line), where all dopants are charged, are screened by the formation of electron-hole puddles. The potential $\phi(\mathbf{r})$ (solid line) obtained in the ground state is restricted to the range $[-\Delta/2 - E_c, \Delta/2 + E_c]$. Puddle formation occurs in tiny regions (gray shading) where $\phi(\mathbf{r})$ exceeds the band edges and is thus above $\Delta/2$ or below $-\Delta/2$. Panel a)-d) shows four one-dimensional cuts through the three-dimensional potential, see text for discussion. Plots are taken from simulations with $L = 50$ (250000 dopants), $\Delta = 10$ and periodic boundary conditions.

$\phi \sim \pm\Delta/2$. Using that $\phi \sim \sqrt{R}$, this strongly suggests that the typical length scale R_g , describing both the screening length and the length scale where the potential changes by $\pm\Delta$, is proportional to Δ^2 . Accordingly, the typical charge density in a volume $V = R_g^3$ is $\rho_g \sim Q_{R_g}/V \sim \sqrt{R_g^3}/R_g^3 = R_g^{-3/2} \sim 1/\Delta^3$. To summarize, this scaling argument suggests

$$R_g \sim \Delta^2 \text{ and } \rho_g \sim \Delta^{-3}. \quad (7)$$

Restoring dimensionfull units, these equations read $R_g \sim N^{-1/3}(\Delta/E_c)^2$ and $\rho_g \sim \pm eN(E_c/\Delta)^3$. We will show below that our numerical results are not consistent with Eq. (7): completely different length scales govern the screening in such Coulomb systems.

The length $\sim \text{energy}^{-2}$ scaling of Eq. (7) arises technically from the properties of the uncorrelated state where charged dopants are randomly placed. For such a model, one can calculate exactly the probability distribution of the potential as function of system size L and one finds, for periodic boundary conditions, $P_{\text{uc}}(\phi) = \exp(-\frac{\phi^2}{2aL})/\sqrt{2\pi aL}$ with $a \approx 4$. This implies that the typical potential is of order \sqrt{L} . The argument above implicitly assumes that this simple random walk-like scaling is carried over to the correlated ground state despite the fact that screening leads to a ‘correlated’ redistribution of charges.

In Fig. 1 we compare several one-dimensional cuts of the potential in the uncorrelated state (dashed lines) and

in the correlated ground state (solid lines) obtained from numerical simulations. The potential fluctuations of the uncorrelated state are much larger than $\pm\Delta/2$ (shown here for $L = 50$) triggering screening. For the correlated ground state, in contrast, the potential fluctuations are strongly reduced and lie within the band gap. Puddles are formed in the tiny regions (shaded in gray) where $|\phi|$ slightly exceeds $\Delta/2$. One finds that in these regions $|\phi| - \Delta/2 \sim E_c$.

While the cut in panel a) shows the expected behavior, the cuts in panels b), c) and d) show more complex phenomena. In panel b), for example, the renormalized potential changes directly from the hole- to the electron puddle on a short distance without the type of fluctuations expected from a random-walk process implicitly assumed in the scaling analysis. Panel c) shows that there is a subtle interplay of physics at large and small length scales while panel d) shows that even large fluctuations of the uncorrelated potential cannot predict puddle formation in the correlated ground state. All these examples show that the simple picture on which the scaling argument is based, may not be able to capture the correlated state correctly.

To obtain more quantitative results, one can study the statistical properties of either the potential $\phi(\mathbf{r})$ or directly of the charge distribution $\rho(\mathbf{r})$, since both are related by the Poisson equation $\nabla^2\phi = -\rho$ (up to the short-distance cutoff a_B introduced above). In the following, we will mainly discuss the charge-charge correlation function $C_{\rho\rho}$. We split this into a local part $\sim \delta(\mathbf{r} - \mathbf{r}')$ and a non-local part $C_{\rho\rho}^{\text{nl}}$:

$$C_{\rho\rho}(\mathbf{r}, \mathbf{r}') = \langle \rho(\mathbf{r})\rho(\mathbf{r}') \rangle = Q_0\delta(\mathbf{r} - \mathbf{r}') + C_{\rho\rho}^{\text{nl}}(\mathbf{r} - \mathbf{r}'), \quad (8)$$

where we used charge neutrality $\langle \rho \rangle = 0$. Here and in the following the expectation value $\langle \cdot \rangle$ denotes a disorder average. After disorder averaging all correlation functions only depend on the distance $r = |\mathbf{r} - \mathbf{r}'|$. Thanks to charge neutrality we know that $\int d^3\mathbf{r} C_{\rho\rho}^{\text{nl}}(\mathbf{r}) = -Q_0$. The weight of the δ -peak Q_0 corresponds to $2N(1 - n_0)$ where n_0 is the fraction of neutral dopants.

From the definition of $C_{\rho\rho}^{\text{nl}}$ and the Poisson equation one can derive a set of exact sum-rules

$$\frac{\langle H_C \rangle}{V} = 2\pi \int ds s^1 C_{\rho\rho}^{\text{nl}}(\Delta, s), \quad (9)$$

$$\frac{\langle H_n \rangle}{V} = n_0 N \Delta = 2\pi \Delta \int ds s^2 C_{\rho\rho}^{\text{nl}}(\Delta, s) + \Delta, \quad (10)$$

$$Q_0 = \frac{\langle Q \rangle}{V} = -4\pi \int ds s^2 C_{\rho\rho}^{\text{nl}}(\Delta, s), \quad (11)$$

$$\langle \phi^2 \rangle = -8\pi^2 \int ds s^3 C_{\rho\rho}^{\text{nl}}(\Delta, s). \quad (12)$$

Here $\langle H_C \rangle$ is the disorder average of the Coulomb energy, $\langle H_n \rangle$ are the single particle energies of the dopants, see Eq. (1), $\langle Q \rangle$ is the number of ionized dopants (not counting the neutral ones), and $\langle \phi^2 \rangle$ is the expectation value of the square of the potential (all expressed in our dimensionless units).

We can use these sum-rules to obtain a more rigorous version of the scaling argument given above. We start from the assumption that the physics of the system is governed by a single length scale. In this case $C_{\rho\rho}^{\text{nl}}(\Delta, s)$ can be written as

$$C_{\rho\rho}^{\text{nl}}(\Delta, s) = \Delta^{-\beta} \overline{C_{\rho\rho}^{\text{nl}}(s/\Delta^\gamma)}. \quad (13)$$

We will show that from this assumption alone Eq. (7) can be derived. Later, we will conclude that the scaling ansatz is *not* valid: more than one length scale governs the physics of our system. For the moment, we will, however, explore the consequences of the scaling ansatz.

The bulk fluctuations of the potential are of the order of the bandgap Δ , see Fig. 1, which implies $\langle\phi^2\rangle \sim \Delta^2$. Furthermore, as the fraction of neutral atoms vanishes for large Δ , $n_0 \rightarrow 0$ for $\Delta/E_c \rightarrow \infty$, the density of charged dopants, Q_0 is of order Δ^0 with only subleading corrections. To leading order we therefore obtain from Eqns. (11) and (12)

$$\Delta^0 \sim \int ds s^2 C_{\rho\rho}^{\text{nl}}(\Delta, s) = \Delta^{-\beta+3\gamma} \int ds s^2 \overline{C_{\rho\rho}^{\text{nl}}(s)}, \quad (14)$$

$$\Delta^2 \sim \int ds s^3 C_{\rho\rho}^{\text{nl}}(\Delta, s) = \Delta^{-\beta+4\gamma} \int ds s^3 \overline{C_{\rho\rho}^{\text{nl}}(s)}. \quad (15)$$

Therefore, the scaling ansatz predicts $\beta = 3\gamma$ and $2 = -\beta + 4\gamma$ or, equivalently, $\gamma = 2$ and $\beta = 6$, implying a length scale $\sim \Delta^2$ and a typical charge density $\sim 1/\Delta^3$. This is just a refined version of the argument presented above in Eq. (7).

From Eq. (9) and Eq. (14) we further deduce that the Coulomb energy density $\langle H_C \rangle / V \sim -\Delta^{-\beta+2\gamma} = -\Delta^{-\gamma}$ ($C_{\rho\rho}^{\text{nl}}$ is negative as it describes screening, for example the accumulation of negative charge around a positive one). This implies that the Coulomb energy is minimized by choosing the screening length $R_s \sim \Delta^\gamma$ as small as possible. However, this minimization competes with the increasing $H_n \sim n_0 N \Delta$, see Eq. (10), and of course has to respect the constraints, in particular Eq.(15).

Below, we will show that the predictions derived above from scaling do not hold. Screening occurs on a much smaller length-scale. Technically, the arguments given above break down because the integral in Eq. (15), $\int ds s^3 C_{\rho\rho}^{\text{nl}}(\Delta, s)$ obtains its dominant contribution not from the length scale $s \sim \Delta^\gamma$ but from a parametrically larger length scale. This happens when the scaling function decays slower than $1/s^4$.

IV. SCREENING IN THE BULK

Instead of studying directly the charge-charge correlation function $C_{\rho\rho}^{\text{nl}}(\Delta, s)$, we find it more convenient to investigate the distance dependence of the ‘screening charge’ defined by

$$Q_s(\Delta, r) = 4\pi \int_0^r ds s^2 C_{\rho\rho}^{\text{nl}}(\Delta, s). \quad (16)$$

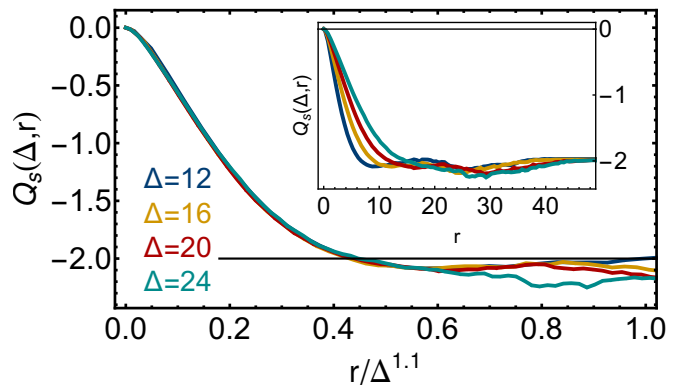


Figure 2. (Color online) Scaling of the screening charge defined in Eq. (16) for different values of the band gap Δ . The best scaling collapse is found for an exponent $\gamma = 1.1$, see Appendix B. The inset shows the unscaled data. Deviations from the scaling behavior can be seen for $r > 0.6 \Delta^{1.1}$. Parameters are $L = 50$ (250000 dopants) for $\Delta = 12, 16$ and $L = 60$ (432000 dopants) for $\Delta = 20, 24$, and we checked that there are no significant finite size effects.

The advantage of this quantity is that it has a direct physical interpretation: it describes the charge accumulated around a dopant within the radius r multiplied with the charge of that dopant and the density of dopants. As negative charges accumulate around a positive charge and vice versa, the screening charge is always negative. Total charge neutrality requires that around a positive (negative) charge exactly the charge -1 ($+1$) accumulates for $r \rightarrow \infty$. As neutral dopants do not contribute, one therefore obtains $Q_s(\Delta, r \rightarrow \infty) = -2N(1 - n_0) = -Q_0$. This also follows directly by integrating Eq. (8) over \mathbf{r} in a charge-neutral system. In our simulations we use boxes of size L with periodic boundary conditions. For $r > L/2$ we therefore have to replace in the integral in Eq. (16) the factor $4\pi s^2$ by $W(s) = \int \delta(s - |\mathbf{r}|) d^3r$. This does not affect the scaling plots discussed below but is useful to check for overall charge neutrality.

We show numerical results for Q_s in Fig. (2). On a rather short length scale (see inset) the screening charge reaches the value $-Q_0 = -2N(1 - n_0) \approx -2$ (the plot uses units where $N = 1$ and the fraction of neutral dopants, n_0 , is less than 2% for all shown values of Δ). The scaling plot (main figure) shows that the length scale ℓ_s , on which the screening occurs, is almost linear in Δ

$$\ell_s \sim \Delta^\gamma, \quad \gamma \approx 1.1 \pm 0.1 \quad (17)$$

In Appendix B we give details on the determination and the error of this quantity. This has to be contrasted with the behavior expected from scaling, which predicts a parametrically much larger screening length of order Δ^2 , and thus at least an order of magnitude larger for the parameters investigated by us. For values of $r \gtrsim 0.4\Delta^\gamma$, the screening charge exceeds $-Q_0 \approx -2$. This implies that there is a substantial amount of overscreening in the system: on average too much charge of opposite sign

accumulates around each charged dopant.

To obtain a scaling collapse, we have rescaled only the r axis but not Q_s . This is equivalent to the statement that the scaling relation derived from Eq. (14), $\beta = 3\gamma$, is valid. To understand the importance of overscreening, let us assume for a moment that perfect screening would occur on the length scale ℓ_s implying a fast decay of $C_{\rho\rho}^{\text{nl}}$ on scales larger than ℓ_s . In this case, one can use Eq. (14) to obtain that the typical size of a potential fluctuation is of the order $\Delta^{\gamma/2} \ll \Delta$, much too small to create the puddles necessary for screening, in contrast to the assumption as long as $\gamma < 2$.

We therefore conclude that the overscreening is ultimately responsible to build up potential fluctuations of sufficient strength. Using the overscreening mechanism, it apparently becomes possible to gain Coulomb energy by bringing opposite charges close to each other and at the same time maintain sufficiently strong potential fluctuations of the order of Δ .

Unfortunately it was not possible to reliably extract a second, larger length scale at which the overscreening crosses over to exact charge compensation. This has to occur when the system size is reached (we have simulated only systems with exact charge neutrality). For large distance the noise level is too high, although each curve is averaged over 800 – 900 disorder realizations. From the numerical results, we can not even exclude that this second length scale is set by the system size in our simulations. Note, however, that the scaling plot of Fig. 2 and thus the determination of ℓ_s is not affected by finite size effects.

We have checked that other observables, for example the potential correlation function or the typical distance of neutral dopants of different type, show similar scaling behaviors, see Appendix A for an example. Most importantly, they all consistently show the importance of the length scale ℓ_s which governs not only screening, but also the length scale on which the dominant short-distance fluctuations of the potential occur. ℓ_s therefore also determines the distance of puddles of opposite charge. We have not found any evidence of a Δ^2 length scale in any observable.

V. SCREENING ON THE SURFACE

Topological insulators differ from ordinary insulators or semiconductors because topology enforces the existence of conducting surface states. These states are of interest in the context of our discussion, because they provide an extra channel for screening. STM measurements of surface states can also be used to obtain quantitative information on the strength and length scale of potential fluctuation at the surface [13].

The surface states of a $3d$ topological insulator can, generically, be described by a Dirac equation, and thus have asymptotically a density of states proportional to the doping level. Their electronic properties can be

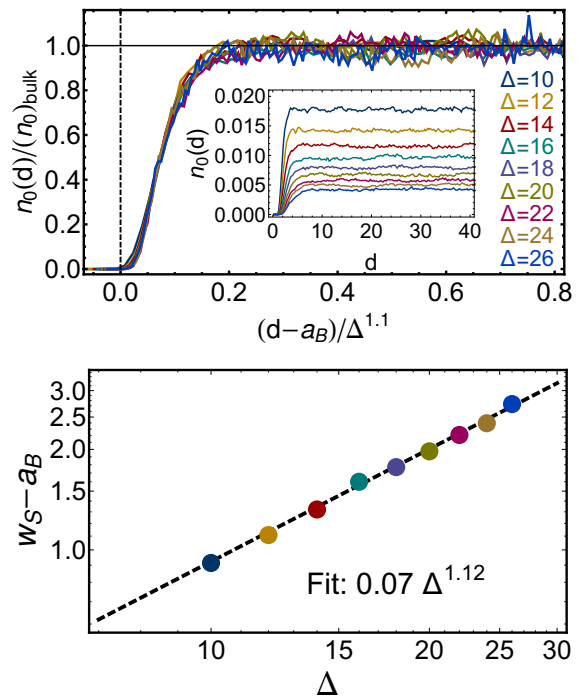


Figure 3. (Color online) Screening from surface-states of a topological insulator suppresses puddle formation close to the surface. Upper panel: Scaling plot of the density of neutral dopants, $n_0(d)$, as a function of the distance d to a metallic surface state ($|\mu^S| \gg E_c/\alpha^2$, $L = 50$). Curves are shifted by $a_B = 1$ since neutralization starts only for $d > a_B$. The inset shows the unscaled data. Lower panel: The width w_S of the surface layer without puddles, defined by $n_0(w_S) = (n_0)_{\text{bulk}}/2$ as a function of Δ . A fit gives an exponent 1.12 very close to the bulk value, see Eq. (17).

characterized by the surface doping μ^S and the effective fine structure constant $\alpha = \frac{e^2}{4\pi\epsilon_{\text{surf}}\epsilon_0\hbar v_F}$, where, in vacuum, $\epsilon_{\text{surf}} = \frac{\epsilon_{\text{bulk}} + 1}{2} \sim 100$. Typical values for α in Bi-based topological insulators are in the range of $\alpha \approx 0.1 \dots 0.2$ (using, e.g., v_F taken from ARPES data [17]). In Ref. [11], Skinner, Chen and Shklovskii develop a detailed analytic theory on how bulk impurity states affect the surface. We will instead investigate the question how the screening from surface states feeds back on bulk properties using some of their results.

If the surface possesses a finite doping, described by a finite chemical surface potential μ^S , it can screen charges on a length scale described by the surface screening length $\ell_s^S \sim v_F/(\alpha|\mu^S|)$. We first consider the limit that ℓ_s^S is smaller than the distance of bulk impurities, $\ell_s^S \lesssim N^{-1/3}$ or, equivalently, $|\mu^S| \gtrsim E_c/\alpha^2$. In this case the surface state of the topological insulator acts effectively like a perfect metal. Then, screening of a dopant with charge q_i at distance z from the surface is described by positioning a mirror charge with charge $-q_i$ at the same distance on the opposite side of the surface. This simple screening mechanism can be implemented in a straightforward way into the model described in Sec. II.

The surface screening will suppress potential fluctuations and the formation of puddles close to the surface. Therefore, all donors will have charge +1, all acceptors have charge -1 and the density of neutral dopants vanishes close to the surface. This physics can be captured by computing the density of neutral dopants, having a charge 0, as a function of distance from the surface

$$n_0(d) = \left\langle \sum_i \delta(d - z_i) \delta_{q_i, 0} \right\rangle, \quad (18)$$

where z_i is the (dimensionless) distance of dopant i from the surface and $\delta_{i,j}$ denotes the Kronecker delta. The inset of Fig. 3 shows $n_0(d)$ for values of Δ ranging from 10 to 26. On a relatively short length scale, the bulk value of $n_0(d)$ is reached. In the lower panel of Fig. 3 we plot the width w_S of the zone, where surface screening suppresses puddle formation, defined by $n_0(w_S) = (n_0)_{\text{bulk}}/2$. After subtracting the offset $a_B = 1$ we obtain a power law relation

$$w_S \sim \Delta^\gamma, \quad \gamma \approx 1.1 \pm 0.2 \quad (19)$$

In Appendix B we give details on the error of this quantity. We also performed simulation with several other values of a_B ($a_B = 0, 0.5, 1.5, 2$) and have checked that subtracting a_B results in the same curve (for a fixed value of Δ). Also the scaling plot in the upper panel of Fig. 3 confirms that w_d governs the size of ‘dead zone’, where puddle formation is suppressed. We obtain for this surface effect the same exponent as for the bulk screening length with remarkable precision. This clearly shows that the same length scale governs both phenomena. The fact that both, the distance of puddles and the length scale on which surface screening suppresses puddle formation, are governed by a length scale much shorter than anticipated from scaling arguments is the main result of this study.

Above we assumed a perfectly metallic surface state, $|\mu^S| \gtrsim E_c/\alpha^2$, which has a screening length that is short compared to the mean distance of dopants $N^{-1/3}$. Using the result given above, that the screening by bulk states sets in only at a parametrically larger scale, $w_S \sim N^{-1/3}(\Delta/E_c)^\gamma$, we can relax this requirement. Our results should be valid as long as the surface screening length $\ell_s^S \sim v_F/(\alpha|\mu^S|)$ is small compared to w_S , or $|\mu^S| \gg v_F/(\alpha w_S) \sim (E_c/\Delta)^\gamma E_c/\alpha^2$.

Here μ^S denotes an effective chemical surface potential. Even if the chemical potential of the surface state is *exactly* at the Dirac point, $\langle \mu^S \rangle = 0$, disorder will induce a finite density of states allowing for screening. Due to the charged dopants metallic puddles will form on the surface which can, in turn, screen bulk charges. To estimate the effect of these surface puddles (not to be confused with puddles in the bulk) we use the results of Ref. [11]. Similar results in the context of graphene have, e.g., been obtained in Refs. [2, 3]. For the computation of the resulting surface screening length ℓ_s^S for $\langle \mu^S \rangle = 0$ the authors of Ref. [11] did not take into account any bulk-screening effects, which is justified as long as $\ell_s^S \ll w_S$.

Under these conditions, Skinner, Chen and Shklovskii [11] found that $|\mu^S| \sim E_c/\alpha^{2/3}$ or $\ell_s^S \sim N^{-1/3}/\alpha^{4/3}$. From the condition $\ell_s^S \ll w_S$, we obtain

$$\left(\frac{\Delta}{E_c}\right)^\gamma > c \left(\frac{1}{\alpha}\right)^{4/3} \quad \text{for } \langle \mu^S \rangle = 0 \quad (20)$$

Using the fit to w_S shown in Fig. 3 and prefactors quoted in Ref. [11], we obtain a rather large dimensionless prefactor $c \approx 9$.

If the condition (20) is fulfilled, the surface state of a topological insulator provides sufficient screening to suppress efficiently the formation of puddles within the distance w_S .

VI. DISCUSSION AND OUTLOOK

We have investigated the influence of charge dopants in (topological) insulators focusing mainly on the role of the screening length ℓ_s generated by the formation of electron-hole puddles. Motivated by the physics of Bi-based topological insulators, we studied the limit where the gap Δ is large compared to the Coulomb energy E_c of neighboring dopants with $\Delta/E_c \sim 100$ as a typical value [6]. The main result is our finding that the dominant length scale for screening is proportional to $(\Delta/E_c)^\gamma$ with $\gamma \approx 1.1 \pm 0.1$.

This length scale also determines how the metallic surface state of a topological insulator affects the bulk puddle formation. This leads to, perhaps, the most important practical consequence of our finding: In sufficiently thin slabs of topological insulators one can use surface screening to suppress the formation of bulk puddles completely. Assuming, for example, $\Delta/E_c \sim 100$ and $N \approx 10^{19} \text{ cm}^{-3}$, we estimate that this mechanism works for slabs thinner than $\sim 100 \text{ nm}$. We therefore predict that for compensation doped Bi-based compounds the bulk conductance will be suppressed considerably (i.e. much faster than to be expected from geometric factors) when the slab becomes thinner than this length scale. More precisely, this prediction rests on the validity of Eq. 20. Therefore large ratios of Δ/E_c and small values of the surface velocity (and thus larger values of α) are preferable.

An important challenge is to find a theory explaining the value of the exponent $\gamma \approx 1.1 \pm 0.1$ describing the relation of screening length and Δ/E_c . Our numerics is consistent with a simple linear relation, $\ell_s \propto \Delta/E_c$, but finding an analytic argument for that has turned out to be difficult due to the long-ranged nature of Coulomb interaction, the highly non-Gaussian distribution of potentials, and the absence of a proper field theory describing the screened state.

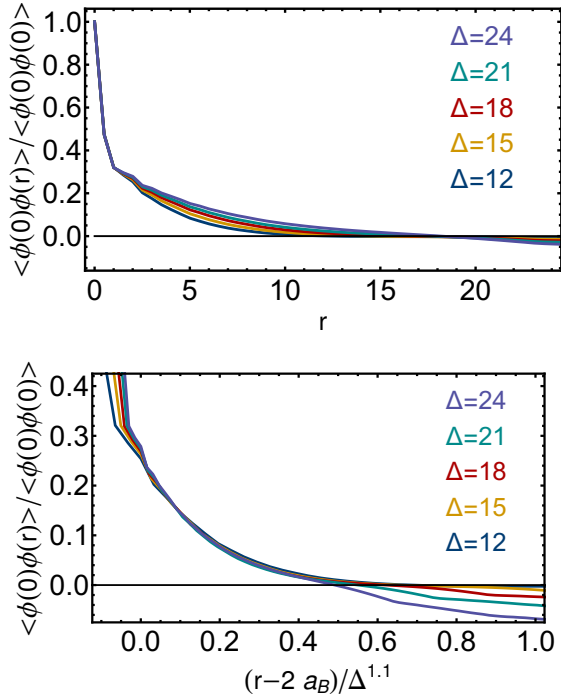


Figure 4. (Color online) The potential correlation function $\langle \phi(\mathbf{r})\phi(0) \rangle$ normalized to $\langle \phi(0)\phi(0) \rangle$ allows to determine the length scale of fluctuations of the potential. Upper panel: Unscaled data. Lower panel: Scaling plot for $\Delta = 12 \dots 24$. For the scaling of the horizontal axis, we first subtract a short-distance cutoff (see text) and then use the scaling of the bulk screening length $\ell_s \sim \Delta^\gamma$ where $\gamma \approx 1.1$, see Eq. (17), see text. Scaling breaks down both at short distances of the order of the cutoff and for larger distances, likely related to a second, longer length scale related to overscreening.

ACKNOWLEDGMENTS

We thank Y. Ando, O. Breuning, N. Borgwardt and M. Grüninger for discussions and collaborations on related work. The numerical simulations have been performed on the CHEOPS cluster at RRZK Cologne. We thank the DFG for financial support within project C02 of CRC 1238.

Appendix A: Correlations of the potential

As show in Fig. 1 the potential in the bulk of a compensation-doped insulator fluctuates in space. It is approximately restricted to the range $[-\Delta/2, \Delta/2]$ and exceeds $\pm\Delta/2$ by an amount of order E_c only in the region where puddles form. The correlation function $\langle \phi(r)\phi(0) \rangle$ shows on which length scale the characteristic potential fluctuations occur.

In Fig. 4 we show $\langle \phi(r)\phi(0) \rangle$ normalized to $\langle \phi(0)\phi(0) \rangle \sim \Delta^2$. At short distances (of the order of the distance of impurities), this is governed by the au-

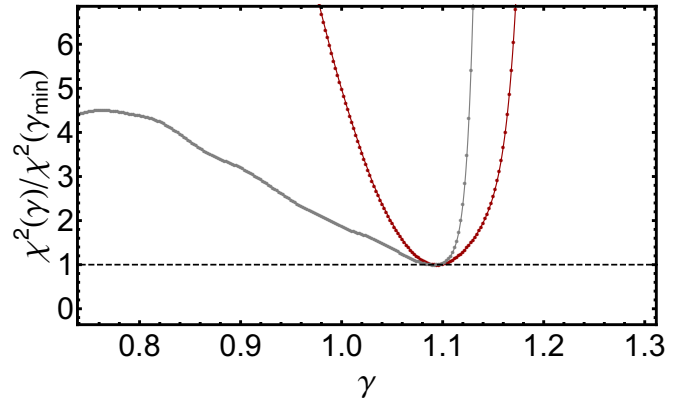


Figure 5. (Color online) The quality of the scaling plots is determined from the square deviation $\chi^2(\gamma)$ defined in Eq. (B1). $\chi^2(\gamma)$ is shown as a function of γ in red and gray for the scaling plot of Fig. 2 and Fig. 3, respectively. For both quantities $\gamma_{\min} \approx 1.1$ is obtained as the best exponent given by the minimum of χ^2 . See the text for a discussion of the error bars.

tocorrelation of the potential of a single charge and decays on a length scale set by a_B . As can be seen in the upper panel of Fig. 4, the normalized correlation function is independent of Δ in this regime. The next-largest length scale, the screening length, on which the correlations decay is more interesting. As expected, we find that this length scale is governed by the bulk screening length $\ell_s \sim \Delta^\gamma$, see Eq. 17. This is shown by the scaling plot in the lower panel of Fig. 4. Clearly the same length scale $\approx 0.2N^{-1/3}(\Delta/E_c)^{1.1}$ (including prefactors) determines the screening radius and the dominant length scale of potential fluctuations. Note that scaling does not hold at the short distances ($\lesssim a_B$ and/or impurity distance $N^{-1/3}$) and that we had to subtract a short distance cutoff to obtain a reasonable scaling collapse.

At larger length scales, the correlation function becomes negative. This physics is, however, *not* governed by ℓ_s as follows from the absence of a scaling collapse in this regime. As discussed in the main text, the physics in the second regime is related to overscreening and occurs on a length scale which we cannot resolve with our numerical simulations.

Appendix B: Determination of γ

The exponent γ governing the screening length ℓ_s as function of Δ/E_c has been determined in our paper from both the r dependence of the screening charge $Q_s(r)$, see Fig. 2, and from the density of neutral impurities close to a metallic surface, see Fig. 3. The exponent can either be obtained from fits (on a log-log scale) of the half-width as function of Δ , see lower panel of Fig. 3, or from the quality of the scaling collapse. To obtain a quantitative value for the latter, we calculate for a set of scaling functions C_i the square deviation $\chi^2(\gamma)$ defined

by

$$\chi^2(\gamma) = \frac{1}{2} \sum_{i,j} \xi_{ij}^2(\gamma), \quad (\text{B1})$$

$$\xi_{ij}^2(\gamma) = \int_0^{r_{\max}} dr |C_i(r/\Delta_i^\gamma) - C_j(r/\Delta_j^\gamma)|^2.$$

r_{\max} was chosen such that all points are in the relevant scaling regime. The resulting χ^2 is shown for both, the screening charge and the suppression of puddle formation at the surface, in Fig.5. From all methods we obtain as

a best estimate for the exponent $\gamma \approx 1.1$.

The error bars are more difficult to estimate as they are mainly determined by systematic and not by statistical errors related to averaging over disorder configurations. A main source of systematic errors is that the screening length $\ell_s \approx 0.2(\Delta/E_c)^{1.1}$ exceeds the average distance of impurities ($= 1$ in our units) only by a factor of 7 for the largest value of Δ used in our simulations. We do not have a reliable method to estimate this systematic error. From the width of the minimum in χ^2 we estimate the error in γ from ℓ_s to 0.1 and from w_s to 0.2. Importantly, the value $\gamma = 1$ is consistent with our numerical results.

-
- [1] A. L. Efros and B. I. Shklovskii, *Electronic Properties of Doped Semiconductors* (Springer Berlin Heidelberg, 1984).
- [2] E. H. Hwang, S. Adam, and S. D. Sarma, Phys. Rev. Lett. **98**, 186806 (2007).
- [3] S. Adam, E. H. Hwang, V. M. Galitski, and S. Das Sarma, Proceedings of the National Academy of Sciences **104**, 18392 (2007), <http://www.pnas.org/content/104/47/18392.full.pdf>.
- [4] J. Martin, Akerman N., Ulbricht G., Lohmann T., Smet J. H., von Klitzing K., and Yacoby A., Nature Physics **4**, 144 (2008).
- [5] Zhang Yuanbo, Brar Victor W., Girit Caglar, Zettl Alex, and Crommie Michael F., Nature Physics **5**, 722 (2009).
- [6] N. Borgwardt, J. Lux, I. Vergara, Z. Wang, A. A. Taskin, K. Segawa, P. H. M. van Loosdrecht, Y. Ando, A. Rosch, and M. Grüninger, Phys. Rev. B **93**, 245149 (2016).
- [7] C. W. Rischau, A. Ubaldini, E. Giannini, and C. J. van der Beek, New Journal of Physics **18**, 073024 (2016).
- [8] Z. Ren, A. A. Taskin, S. Sasaki, K. Segawa, and Y. Ando, Phys. Rev. B **84**, 165311 (2011).
- [9] B. Skinner, T. Chen, and B. I. Shklovskii, Phys. Rev. Lett. **109**, 176801 (2012).
- [10] B. Skinner, T. Chen, and B. I. Shklovskii, J. Exp. Theor. Phys. **117**, 579 (2013).
- [11] B. Skinner and B. I. Shklovskii, Phys. Rev. B **87**, 075454 (2013).
- [12] O. Breunig, Z. Wang, A. A. Taskin, J. Lux, A. Rosch, and Y. Ando, accepted by Nat. Comm. (2017).
- [13] H. Beidenkopf, Roushan, Pedram, Seo, Jungpil, Gorman, Lindsay, Drozdov, Ilya, Hor Yew San, Cava R. J., and Yazdani, Ali, Nature Physics **7**, 939 (2011).
- [14] S. A. Basylo, P. J. Kundrotas, V. A. Onischouk, E. E. Tornau, and A. Rosengren, Phys. Rev. B **63**, 024201 (2000).
- [15] J. Lux, *Fluctuations in and out of equilibrium: Thermalization, quantum measurements and Coulomb disorder* (PhD thesis, Universität zu Köln, 2016).
- [16] B. Shklovskii and A. Efros, Sov. Phys. JETP **35**, 610 (1972).
- [17] Xia Y., Qian D., Hsieh D., Wray L., Pal A., Lin H., Bansil A., Grauer D., Hor Y. S., Cava R. J., and Hasan M. Z., Nat Phys **5**, 398402 (2009), 10.1038/nphys1274.